Korean J. Chem. Eng., 40(5), 1151-1167 (2023)
DOI: 10.1007/s11814-022-1300-3

pISSN: 0256-1115
eISSN: 1975-7220

Experimental, modeling and RSM optimization of CO_2 loading for an aqueous blend of diethylenetriamine and 3-dimethyl amino-1-propanol

Akhil Kumar Gupta, Ashish Gautam, and Monoj Kumar Mondal†

Department of Chemical Engineering and Technology, Indian Institute of Technology (Banaras Hindu University), Varanasi 221005, Uttar Pradesh, India

(*Received 9 June 2022 • Revised 18 September 2022 • Accepted 23 September 2022*)

Abstract−Post-combustion CO_2 capture by aqueous amine solvent is one of the most promising methods for mitigating the presence of CO_2 in the environment. In this work, a novel amine blend of Diethylenetriamine and 3-Dimethyl amino-1-propanol was selected. Experiments were performed in the temperature range of 293.15-323.25 K, mole fraction of diethylenetriamine in the range of 0.05-0.2, partial pressure of CO_2 in the range of 10.13-25.33 kPa and solution concentration in the range of 1-3 mol·L^{-1}. Effects of these parameters on equilibrium CO_2 loading were judged at various operating conditions. An empirical model was developed for the calculation of equilibrium CO_2 loading in the aqueous amine blend. The heat of absorption of CO_2 for this amine blend was found to be −65.22 kJ·mol^{-1}. Response surface methodology (RSM) was used for optimization and a quadratic model was selected. The analysis of variance was used to prove the significance of the selected model. Three-dimensional diagrams and contour plots of independent variables were also shown. Optimum CO_2 loading by RSM was found to be 1.068 mol CO_2·mol $amine^{-1}$ at temperature 294.15 K, mole fraction of diethylenetriamine 0.20, solution concentration 1.3 mol/l, and partial pressure of CO_2 24.22 kPa.

Keywords: CO_2 Loading, Diethylenetriamine and 3-Dimethylamino-1-Propanol Blend, Empirical Model, Heat of Absorption and Desorption Heat Duty, RSM for Optimization and ANOVA

INTRODUCTION

It is quite known that greenhouse gas emissions like CO_2, CH_4, N_2O, SO_X, NO_X, and HFCS are responsible for global warming and climate issues. Among all of these gases, CO_2 gas emissions due to various human activities, like the burning of conventional fossil fuels, play a major role in the greenhouse effect [1,2]. In this chain, coal-fired thermal power plants contribute one-third of overall CO_2 emissions worldwide [2,3-7] and are a problematic concern in the present scenario. Cement industries [8], food industries [9], iron and steel industries [10], petrochemical industries [11], and petroleum refineries [12] are the major sectors responsible for CO_2 emissions. Approximately 80% of CO_2 emissions have increased from 21 to 38 gigatons (Gt) from the years 1970 to 2004.

Carbon capture & storage (CCS) is an important key solution to overcoming these CO_2 emission challenges. There are three techniques especially available for this task: pre, post, and oxy-combustion. Any of these techniques is adopted by using numerous available methodologies, i.e., absorption (either physical or chemical), adsorption, membrane technology, cryogenic separation, and chemical looping combustion (CLC) [13-19] for CO_2 capture. Out of all, post-combustion CO_2 capture by the chemical method using absorption is a highly mature technique [1,20-22]. Amines have been used widely for capturing CO_2, i.e., a single alkanolamine-based solvent, i.e., monoethanolamine (MEA), has been used as a chemical solvent to capture CO_2 for many decades. But there have been some drawbacks with MEA: Limited CO_2 loading and high regeneration costs, which has attracted researchers to work on the different amines and amine blends to mitigate these problems. It was found that regeneration costs for amines are 70-80% of the overall operational cost [2,22-25], and this made researchers to think about other options, such as different amines and amine blends. Various amine blends are prepared by mixing high-kinetics solvents (Activators) with low-kinetics solvents (Promoters). Primary and secondary amines are classified as activators ($\Delta H_{rxn} \approx 80$ kJ $mol^{-}_{CO_2}$), while tertiary or hindered amines are known as promoters ($\Delta H_{rxn} \approx 60$ kJ $mol^{-}_{CO_2}$). Amine solvent blends are necessary because of their fast kinetics, high absorption capacity, low regeneration costs, high thermal stability, less corrosion risk, and low environmental impact [6]. Cyclic polyamines (Piperazine and piperazine derivatives) and non-cyclic polyamines (1,6-hexamethyldiamine and 1,3-diamino-2-propanol) were also tested for removal of CO_2 for different gas streams under different operating conditions [26,53].

A linear polyamine, diethylenetriamine (DETA) contains three amino groups present in its structure and has a fast absorption rate, high mass transfer, large cyclic capacity. It requires lower regeneration energy towards CO_2 as compared with conventional monoethanolamine (MEA) solvents [2,20,22,27-31]. 3-DMA-1-P is a tertiary amine, it has higher CO_2 loading and a higher reaction rate as compared with conventional MDEA and TEA [32,33]. Many researchers have experimented with DETA and 3-DMA-1-P separately and obtained promising results against conventional amines.

Gao et al. [2] performed an absorption and desorption experiment using DETA solvent in a pilot plant and compared its per-

†To whom correspondence should be addressed.
E-mail: mkmondal13@yahoo.com

formance with MEA solvent [22,23]. Operating parameters were solvent and flue gas flow rate, DETA concentration, and regeneration temperature and, finally, their consequences were investigated. Liu et al. [31] further examined the absorption capacity, absorption rate, absorption heat, and regeneration energy consumption of six different amine blends, and lee et al. found these for the blend of DEEA and DETA [55]. The various mass ratios of the PZ/DETA amine blend (superior properties) were prepared, and among them, the most appropriate ratio was reported. Initially, Hartono et al. [27] and Yu et al. [1] revealed the chemistry and properties of DETA amine and reported that DETA has higher CO_2 reactivity, absorption capacity, and boiling point but lower vapor pressure as compared with MEA solvent. The apparatus modification was done by Yu et al. [1] and Wu et al. [34], who performed a CO_2 absorption experiment in the rotating packed-bed reactor.

3-DMA-1-P had more CO_2 loading and had the potential to replace conventional tertiary amines. Li et al. [15] and Afkhamipour et al. [17] calculated the equilibrium CO_2 loading in 3-DMA-1-P and other amine solvents and also developed a thermodynamic model, which was the most promising model related to their experimental work. Kadiwala et al. [35], Bernhardsen et al. [36], and Nath et al. [37] calculated the kinetics of CO_2 with density, viscosity, reaction mechanism, etc. of 3-DMA-1-P and other amine solvents by using stopped-flow techniques. Singh et al. [38] selected 3-DMA-1-P and 1,5-Diamino-2-methyl pentane amine blend and calculated the CO_2 loading, absorption enthalpy, and also developed the empirical model. Belabbaci et al. [39] calculated the vapor-liquid equilibrium (VLE) data of 2-amino-2-methyl-1-propanol (AMP)+H_2O, 3-dimethylamino-1-propanol (3-DMA-1-P)+H_2O at different operating temperatures. So the individual fine properties of DETA and 3-DMA-1-P amine solvents can be more advantageous in their blend of DETA+3-DMA-1-P.

To use optimization software of response surface methodology (RSM), the experimental work is correlated either with the first- or second-order regression models [40], and optimization [41,42] is done either by using central composite design (CCD) or Box-Behnken design (BBD) methods.

BBD analysis was used to create a first-order regression model, and also used to assess the model's fitness by generating the sample points [40]. Most of the model designs used in RSM software are represented in quadratic equations because they are a highly trusted analysis method and involve all the independent variables. The superior acceptable accuracy with the low number of experiments in BBD design sets it apart from the other design methods available in RSM software [43,44]. Many engineering problems have been solved using optimization by BBD design, and Nuchitprasittichai and Cremaschi [45] used it to optimize the CO_2 capture process with aqueous amine as one of the examples. In the same manner, CCD is also one of the statistical design tools used in optimization techniques. It provides the run samples in the form of 2^n factorial consisting of 2n axial runs with some central runs as well [46]. The response of CCD can be analyzed with the help of analysis of variance (ANOVA). The factors like the degree of freedom (df), P value, and F value were analyzed in the ANOVA to judge the model's significance [47,48]. The majority of the literature has optimized with the CCD design [46-51]. In the last decade, only a few kinds of research have been done with the help of the RSM method in the field of CO_2 capture.

In this present work, with the help of available literature and by keeping in mind the marvelous effects and properties of each amine on CO_2 loading, a novel aqueous amine blend of DETA+3-DMA-1-P was prepared for the estimation of CO_2 loading. The reaction chemistry of the amine blend system is being suggested in order to get an idea about equilibrium CO_2 loading in aqueous amine blend. The equilibrium CO_2 loading in the aqueous amine blend solution of DETA+3-DMA-1-P was measured at various operating conditions, such as solution concentration varied from 1-3 mol/l, DETA (Activator) mole fraction in the amine solution changed from 0.05-0.2, partial pressure of CO_2 ranging from 10.13-25.33 kPa, temperature range of 293.15-323.15 K, and the entire experiment was performed for up to 10 hours to get complete saturation. An empirical model was developed for the estimation of CO_2 loading to authenticate the theoretical and experimental results. The heat of absorption of this selected amine blend was estimated with the help of the Gibbs-Helmholtz equation, and it was found to be $-65.22\ kJ{\cdot}mol^{-1}$, which is less than that of conventional monoethanolamine ($-85.13\ kJ{\cdot}mol^{-1}$). Therefore, this amine blend was selected for further experimental work. The experimental equilibrium CO_2 loading data for this work was collated with the available literature. Response surface methodology (RSM) was finally used, and the CCD technique was employed to get optimized results of independent variable used in the experimental work.

EXPERIMENTAL DESCRIPTION

1. Chemicals Used

DETA and 3-DMA-1-P amines were collectively used as their amine blend for calculating equilibrium CO_2 loading for experimental purposes. Various other chemicals like monoethanolamine (MEA), hydrochloric acid (HCL), CO_2, H_2O, and N_2 with their important specifications like CAS No., molecular structure, boiling point, density, purity, and supplier are shown in Table 1. DETA ($C_4H_{13}N_3$) and MEA (C_2H_7NO) chemicals were purchased from Sigma-Aldrich St. Louis, (USA); 3-DMA-1-P ($C_5H_{13}NO$) chemical was purchased from Tokyo Chemical Industry Co. Ltd, Tokyo, (Japan).

2. Characterization

Initially, the amine blends of DETA+3-DMA-1-P were prepared with the help of double-distilled water which was prepared in the laboratory by using a double distillation process. The pH of the solution so formed was analyzed with a digital pH meter (model Systronics-335 with an accuracy of ±0.01) after being calibrated with a standard buffer solution. The CO_2 and N_2 gases were supplied by Linde India Ltd. The flow rate of gases was controlled by using a digital gas flow controller (MC-500SCCM-D, Alicat Scientific, New Delhi, India, accuracy ±0.6%). A laboratory-scale borosilicate absorption column was used for absorbing CO_2 in amine solution during the entire experiment. A portable infrared-based flue gas analyzer (Gasboard-3800P, Wuhan, China, CO_2 range 0-100% V/V) was used to check the concentration of CO_2 in the gaseous mixture of pre- and post-absorption column with ±0.1% accuracy. The absorber column was placed inside the water bath,

Table 1. The different specifications of chemicals used in this specific work

Chemical used	CAS No.	Structure	BP (°C)	ρ (Kg/m^3)	Molecular weight (g/mol)	Purity (in mass fraction)	Make
Diethylenetriamine (DETA)	111-40-0	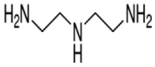	199-209	955.0	103.17	0.99	Sigma-Aldrich
3-(Dimethylamino)-1-propanol (3-DMA-1-P)	3179-63-3	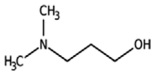	159.0	886.0	103.17	0.99	TCI, Tokyo, Japan
Monoethanolamine (MEA)	141-43-5	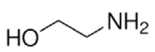	170	1,011.7	61.08	0.99	Sigma-Aldrich
Hydrochloric acid (HCL)	7647-01-0	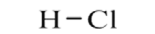	−85.05	1200	36.46	0.37	Merck
Carbon dioxide (CO_2)	124-38-9	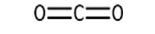	−78.46	1.98	44.01	0.99	Linde India Limited
Nitrogen (N_2)	7727-37-9		−195.8	1.25	14.00	0.99	Linde India Limited
Distilled Water (H_2O)	7732-18-5	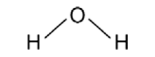	100	998.2	18.02	0.99	Prepared at Lab scale

having an incubator shaker and temperature controller to obtain the desired temperature within the least variation of ±0.1%. Finally, the total desired concentration of the amine blend solution was checked and analyzed with titration by HCl solution. The titration apparatus uses magnetic beads for stirring purposes; ultimately, the amount of CO_2 was calculated.

3. Description of Experimental Setup

The complete description of the experimental setup can be seen under the supporting data section with the figure of the experimental setup Fig. S1.

4. Equilibrium CO_2 Loading Estimation

The equilibrium CO_2 loading in the amine blend of DETA and 3-DMA-1-P solution was performed with slight modifications to the setup proposed by Singh et al. [38]; its schematic representation is shown in Fig. S1. The high potential of 3-DMA-1-P amine to capture CO_2 was shown in the literature by many authors [15, 17,32,35-39]. This work is mainly divided into three main categories: feed gas stream, absorber section, and CO_2 estimation.

Feed gas stream under controlled flow rate and pressure passed through the mixing chamber and bubbled continuously into the absorption column (Fig. S1) until complete saturation of amine blend solution occurred. This saturation occurs when inlet and outlet concentrations of CO_2 gas become equal. The absorption experiment was performed at a temperature range of 293.1-323.25 K and atmospheric pressure. The CO_2-loaded amine blend solution was taken out from the absorption column and directly titrated with 1 M HCl solution, and methyl orange (0.1 wt%) was used as an indicator. Since the CO_2-loaded solution is carbamate-saturated, therefore, the water displaced during titration helps evaluate equilibrium CO_2 loading [38]. A fixed, known volume of saturated solution at room temperature and pressure was used to perform this task, and the whole titration setup is known as the Chittick apparatus. Ultimately, CO_2 loading was calculated in moles of CO_2 per mole of amine blend used. To attain accuracy, the experiments were conducted thrice, and the average value of the equilibrium CO_2 loading was finally reported.

5. Reaction Chemistry of the CO_2+DETA+3-DMA-1-P System

When the DETA and 3-DMA-1-P amine blend reacts with the CO_2, the following set of chemical reactions take place in the liquid phase. Chemical equilibrium is shown by the equilibrium constants. The individual sets of chemical reactions are also shown in detail by the authors [15,22,27,28,32,38].

Physical solubility:

$$CO_2(g) \overset{H_{CO_2}}{\longleftrightarrow} CO_2(aq.) \quad \text{(R1)}$$

H_2O dissociation:

$$H_2O \overset{K_1}{\longleftrightarrow} H^+ + OH^- \quad \text{(R2)}$$

Bicarbonate ion formation:

$$CO_2 + H_2O \overset{K_2}{\longleftrightarrow} HCO_3^- + H^+ \quad \text{(R3)}$$

Carbonate ion formation:

$$HCO_3^- \overset{K_3}{\longleftrightarrow} CO_3^{2-} + H^+ \quad \text{(R4)}$$

DETA intermediate reactions:

$$CO_2 + DETA + H_2O \overset{K_4}{\longleftrightarrow} DETACOO^- + H_3O^+ \quad \text{(R5)}$$

$$CO_2 + DETA + OH^- \overset{K_5}{\longleftrightarrow} DETACOO^- + H_2O \quad \text{(R6)}$$

$$CO_2 + DETA + HCO_3^- \overset{K_6}{\longleftrightarrow} DETACOO^- + H_2CO_3 \quad \text{(R7)}$$

Bicarbonate and DETA ion formation:

$$CO_2 + DETA + CO_3^{2-} \overset{K_7}{\longleftrightarrow} DETACOO^- + HCO_3^- \quad \text{(R8)}$$

DETA and CO_2 overall reaction:

$$CO_2 + 2DETA \overset{K_8}{\longleftrightarrow} DETACOO^- + DETAH^+ \quad \text{(R9)}$$

3-DMA-1-P reaction:

$$3\text{-DMA-1-PH}^+ \overset{K_9}{\longleftrightarrow} 3\text{-DMA-1-P} + H^+ \quad \text{(R10)}$$

$$CO_2 + 3\text{-DMA-1-P} + H_2O \overset{K_{10}}{\longleftrightarrow} 3\text{-DMA-1-PH}^+ + HCO_3^- \quad \text{(R11)}$$

where H_{CO_2} is Henry's law constant, K_1-K_{11} represents equilibrium

Table 2. Resemblance of CO_2 loading data obtained from experiments and literature in aqueous MEA solution of 4.91 mol·kg^{-1} at specified conditions of temperature, pressure and relative deviation between experimental and literature data[a]

T (K)	P_{CO_2} (kPa)	γ_{exp} (mol CO_2·mol amine^{-1})	γ_{lit} (mol CO_2·mol amine^{-1})	RD%	Reference
313.15	8.09	0.546	0.557	2.01	Jou et al. [52]
313.15	19.12	0.603	0.585	2.98	Tong et al. [53]
313.15	12.80	0.535	0.512	4.30	Shen et al. [54]

[a]Standard uncertainty u for the total MEA solution molality, u(C)=0.001 mol·kg^{-1}, for the CO_2 partial pressure in the inlet gas stream, u(p_{CO_2})=0.05 kPa, for temperature u(T)=1 K, for CO_2 loading u(γ)=0.002 mol CO_2·mol amine^{-1}.

Table 3. Experimental CO_2 loading (γ_{exp}) and calculated CO_2 loading (γ_{cal}) data of aqueous 3-DMA-1-P and DETA absorbent blend at different operating conditions, such as CO_2 partial pressure p_{CO_2} (in kPa), weight fraction of DETA in the amine mixture m_{DETA}, total amine blend concentration C (in mol·L^{-1}), and temperature T (in K)

Run	Operating parameters				γ_{exp} (mol co_2/mol amine)	γ_{cal} (mol co_2/mol amine)	RD%
	T (K)	m_{DETA}	C (mol/L)	P_{CO_2} (kPa)			
1	293.15	0.05	1	20.27	0.935	0.894	4.40
2	293.15	0.10	1	20.27	0.977	0.978	0.10
3	293.15	0.15	1	20.27	1.019	1.035	1.60
4	293.15	0.20	1	20.27	1.060	1.066	0.60
5	303.15	0.20	1	20.27	0.993	1.006	1.35
6	313.15	0.20	1	20.27	0.934	0.927	0.75
7	323.15	0.20	1	20.27	0.815	0.828	1.60
8	313.15	0.05	1	20.27	0.751	0.756	0.70
9	313.15	0.10	1	20.27	0.837	0.839	0.24
10	303.15	0.10	1	20.27	0.898	0.918	2.23
11	323.15	0.10	1	20.27	0.729	0.740	1.51
12	313.15	0.15	1	20.27	0.903	0.896	0.80
13	313.15	0.20	1	10.13	0.798	0.794	0.50
14	313.15	0.20	1	15.20	0.891	0.862	3.25
15	313.15	0.20	1	25.33	0.973	0.988	1.54
16	293.15	0.20	2	20.27	1.003	1.021	1.80
17	303.15	0.20	2	20.27	0.956	0.961	0.52
18	313.15	0.20	2	10.13	0.739	0.749	1.35
19	313.15	0.20	2	15.20	0.841	0.817	2.85
20	313.15	0.20	2	20.27	0.905	0.882	2.54
21	313.15	0.20	2	25.33	0.959	0.943	1.70
22	323.15	0.20	2	20.27	0.746	0.784	5.10
23	313.15	0.05	2	20.27	0.717	0.711	0.84
24	313.15	0.10	2	20.27	0.798	0.794	0.50
25	313.15	0.15	2	20.27	0.874	0.851	2.64
26	293.15	0.20	3	20.27	0.939	0.970	3.30
27	303.15	0.20	3	20.27	0.905	0.910	0.55
28	313.15	0.20	3	20.27	0.876	0.831	5.15
29	323.15	0.20	3	20.27	0.697	0.732	5.02
30	313.15	0.05	3	20.27	0.631	0.660	4.60
31	313.15	0.10	3	20.27	0.733	0.743	1.40
32	313.15	0.15	3	20.27	0.824	0.800	2.91
33	313.15	0.20	3	10.13	0.680	0.698	2.65
34	313.15	0.20	3	15.20	0.789	0.766	2.92
35	313.15	0.20	3	25.33	0.917	0.892	2.75
						AAD%=	2.10

constant, and R1-R11 shows the equation labels of each of the chemical reactions.

RESULTS AND DISCUSSION

1. Equilibrium CO_2 Loading in the Amine Blend of 3-DMA-1-P+DETA

The equilibrium CO_2 loading in an aqueous amine absorbent blend of 3-DMA-1-P and DETA was measured at a CO_2 partial pressure (p_{CO_2}) ranging from 10.13-25.33 kPa, the total concentration of aqueous amine blend (C) ranging from 1-3 mol·L^{-1}, temperature range of 293.15-323.15 K, and the weight fraction of activator DETA (m_{DETA}) ranging from 0.05-0.20. All experiments were conducted within the specified conditions, as stated above, at atmospheric pressure. The experimental data for CO_2 loading (γ_{exp}) is listed in Table 3. The CO_2 loading in these experimental runs is expressed as moles of CO_2 absorbed in the absorbent blend per mol of total amine blend (mol CO_2·mol $amine^{-1}$). To authenticate the CO_2 loading data, the experimental setup was corroborated by measuring the equilibrium CO_2 loading in MEA solution at the specific given conditions provided in the literature, and a relative deviation was also calculated between the present experimental data and the data available in the literature.

Table 2 shows that the experimental and literature data point analyses agree with each other. It means that the experimental setup is good enough to carry out the CO_2 loading measurement for our present amine blend of 3-DMA-1-P+DETA.

In this work, the equilibrium CO_2 loading in 3-DMA-1-P+DETA was measured at different operating parameters (T, p_{CO_2}, C, m_{DETA}), and the effect of the change in operating conditions on CO_2 loading is well listed in Table 3. The reason for the change in CO_2 loading on changing operating conditions is discussed in the next segments.

1-1. Effect of Weight Fraction of Activator DETA in the Amine Blend of DETA+3-DMA-1-P on Equilibrium CO_2 Loading

Fig. 1 depicts the effect of the weight fraction of activator DETA in the absorbent blend (3-DMA-1-P+DETA) on equilibrium CO_2 loading (mol CO_2·mol $amine^{-1}$) at different total blend concentrations (i.e., 1, 2, and 3 mol·L^{-1}). In this consideration, other operating parameters, like temperature (313.15 K), and partial pressure of CO_2 (20.27 kPa) were kept constant.

It is evident from the plot that on increasing the concentration of DETA in the amine blend (3-DMA-1-P+DETA), the equilibrium CO_2 loading in the amine blend increases, and the maximum loading was obtained at 0.20 weight fraction of DETA. It is well known from the literature [55] that more amino groups contribute to enhancing the equilibrium CO_2 loading in the chemical mixture.

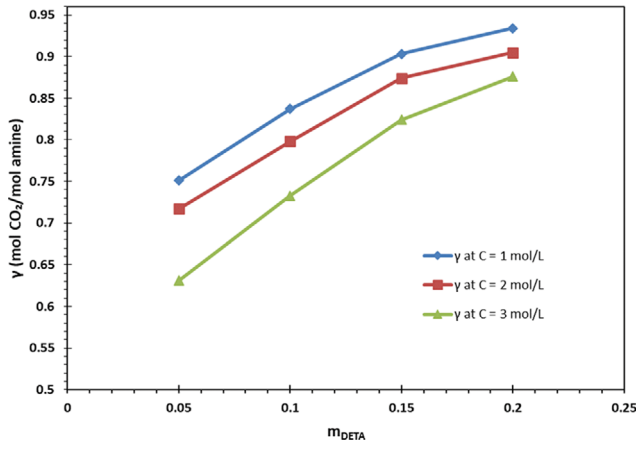

Fig. 1. Effect of weight fraction of DETA (m_{DETA}) in the solution of 3-DMA-1-P+DETA+H_2O on the equilibrium CO_2 loading in the liquid phase (γ) at 1, 2, and 3 molar concentration of total amine blend at T 313.15 K, p_{CO_2} 20.27 kPa.

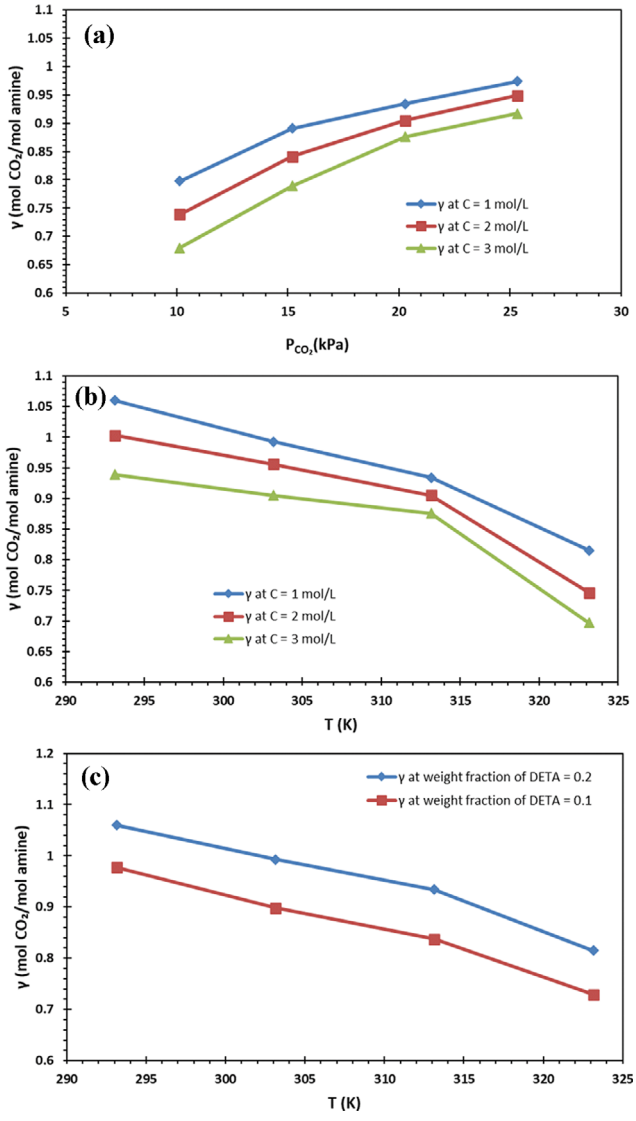

Fig. 2. Effect of (a) partial pressure of CO_2 in inlet gas stream (p_{CO_2}) on equilibrium CO_2 loading in amine solution (γ) at 1, 2, and 3 molar concentration of total amine blend at T 313.15 K, m_{DETA} 0.20, (b) temperature on equilibrium CO_2 loading at different concentrations of total amine blend (1, 2 and 3 mol·L^{-1}) over the temperature range of 293.15-323.15 K at a fixed p_{CO_2} 20.27 kPa and m_{DETA} 0.20, (c) temperature on CO_2 loading at DETA weight fraction of 0.10 and 0.20 at constant p_{CO_2} 20.27 kPa and C 1 mol·L^{-1}.

Therefore, mostly primary and secondary amines exhibit equilibrium CO_2 loading up to 0.5 mol CO_2·mol amine^{-1} and that of tertiary amines up to 1 mol CO_2·mol amine^{-1}. DETA consists of two primaries and one secondary amine group attached to its chemical structure, which provides more reactive sites for the acid gas (CO_2). To further promote CO_2 dissolution in the amine blend, DETA in addition to 3-DMA-1-P (tertiary amine), works as a promising absorbent blend for capturing CO_2. The greater the concentration of DETA in the amine mixture, the more equilibrium CO_2 loading is achieved in the amine blend, and it can be seen from the plot that as the weight fraction of DETA increases, equilibrium CO_2 loading also increases.

1-2. Effect of Partial Pressure of CO_2 and Temperature of the Amine Blend of DETA+3-DMA-1-P on Equilibrium CO_2 Loading

Fig. 2(a) shows the effect of partial pressure of CO_2 in the simulated flue gas stream on the equilibrium CO_2 loading at different concentrations of total amine blend (i.e., 1, 2, and 3 mol·L^{-1}) at a fixed temperature of 313.15 K and a fixed DETA weight fraction of 0.20. Gas absorption in a liquid mixture is well-supported at increased pressure and reduced temperature. Liquids and solids show practically no change in solubility with changes in pressure, but gases do. According to Henry's law, gas solubility in any liquid is directly proportional to the partial pressure of that gas lying above the surface of the solution or liquid at a constant temperature. As the partial pressure of CO_2 gas increases, more gas molecules are forced from the bulk gas phase into the aqueous amine solution, thus increasing the number of gas molecules that dissolve in the solution, and greater amounts of bicarbonates, carbonates, and carbamates form. It can be seen from the plot that by increasing the partial pressure of CO_2 in the gas stream, there is an increase in the equilibrium CO_2 loading in the amine blend because of an increase in gas phase mass-transfer increase due to driving force rise from the bulk gas phase to the gas-liquid interface.

Fig. 2(b) shows the effect of temperature on equilibrium CO_2 loading at the different values of total blend concentration over a wide range of temperatures (293.15-323.15 K) and keeping the partial pressure of CO_2 and DETA weight fraction to be constant at 20.27 kPa and 0.20, respectively. This decrease in equilibrium CO_2 loading with increasing temperature is in agreement with information reported by Kundu et al. [56] and Bajpai et al. [57]. As equilibrium CO_2 loading increases, dynamic equilibrium is established in the dissolution process, and Le Chatelier stated that in the exothermic dissolution process, gas solubility declines as the temperature increases. Because of increased temperature, the gas-liquid equilibrium shifts in the reverse direction; also, gas solubility in the solution is favored at reduced temperature and increased pressure. At high temperature, chemical bonds are weakened and ultimately broken off, which reduces the equilibrium CO_2 loading. From the plot, it can be seen that up to 313.15 K, there is a moderate decrease in CO_2 loading, and after this, a sharp decrease in equilibrium CO_2 loading. Also, it is evident from the graph that as the concentration of the total amine blend is increased, equilibrium CO_2 loading declines over a wide range of temperatures.

Fig. 2(c) shows the variation in equilibrium CO_2 loading in an aqueous amine mixture with a change in temperature over the range of 293.15-323.15 K at DETA weight fractions of 0.10 and 0.20 while keeping the other operating parameters, such as total amine blend concentration (1 mol·L^{-1}) and partial pressure of CO_2 (20.27 kPa) to be constant.

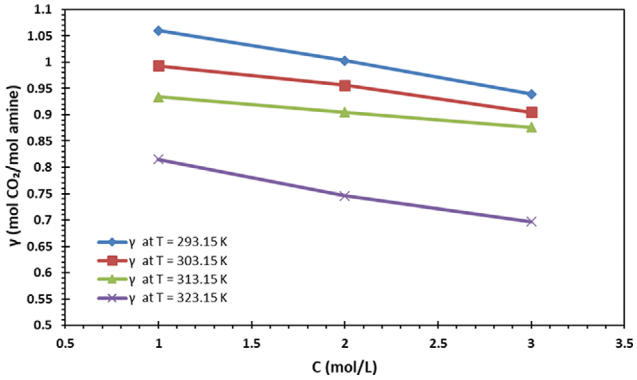

Fig. 3. Variation in equilibrium CO_2 loading with change in total amine blend concentration from 1-3 mol·L^{-1} at various temperature ranges of 293.15-323.15 K at constant p_{CO_2} 20.27 kPa and m_{DETA} 0.20.

1-3. Effect of Total Amine Blend (DETA+3-DMA-1-P) Concentration on Equilibrium CO_2 Loading

Fig. 3 indicates that there is a continuous decrease in equilibrium CO_2 loading with increasing concentration of amine blend from 1-3 mol·L^{-1} at various temperatures (293.15, 303.15, 313.15, and 323.15 K) by keeping the fixed partial pressure of CO_2 at 20.27 kPa and the fixed weight fraction of DETA at 0.20. At high values of concentration, liquid phase resistance increases, and conversion of carbamate to bicarbonate occurs to a very small extent; for this reason, equilibrium CO_2 loading decreases on increasing the total amine blend concentration.

2. Effect of Time on CO_2 Absorption for the Amine Blend DETA+3-DMA-1-P

Fig. 4(a) shows the variation in concentration of CO_2 in the liquid phase with respect to the time consumed in absorption for a specific range of weight fraction of activator (DETA), from 0.05-0.20 at a fixed temperature of 313.15 K, CO_2 partial pressure of 20.27 kPa and total amine blend concentration of 1 mol·L^{-1}. The change in moles of CO_2 absorbed was analyzed at the different compositions of the absorbent blend (different values of DETA and 3-DMA-1-P) at a fixed blend concentration of 1 mol·L^{-1}. It is evident from the graph that moles of CO_2 absorbed in amine solution first increases with time and tends to be constant after some time. It shows that the CO_2 gas is no more soluble in the amine blend, and total amine mixture tends to attain saturation stage for final gas-liquid equilibrium.

Fig. 4(b) shows the increase in CO_2 loading with time at distinct values of partial pressure of CO_2 in the simulated gas stream, i.e., 10.13-25.33 kPa at a constant weight fraction of DETA 0.20 in the amine mixture, the temperature of 313.15 K, and a total amine blend concentration of 1 mol·L^{-1}. It can be seen from the plot that CO_2 loading is decreased as the partial pressure of CO_2 is reduced from 25.33-10.13 kPa.

Fig. 4(c) shows the change in CO_2 loading with respect to time at different values of total amine blend concentration (1, 2, and 3

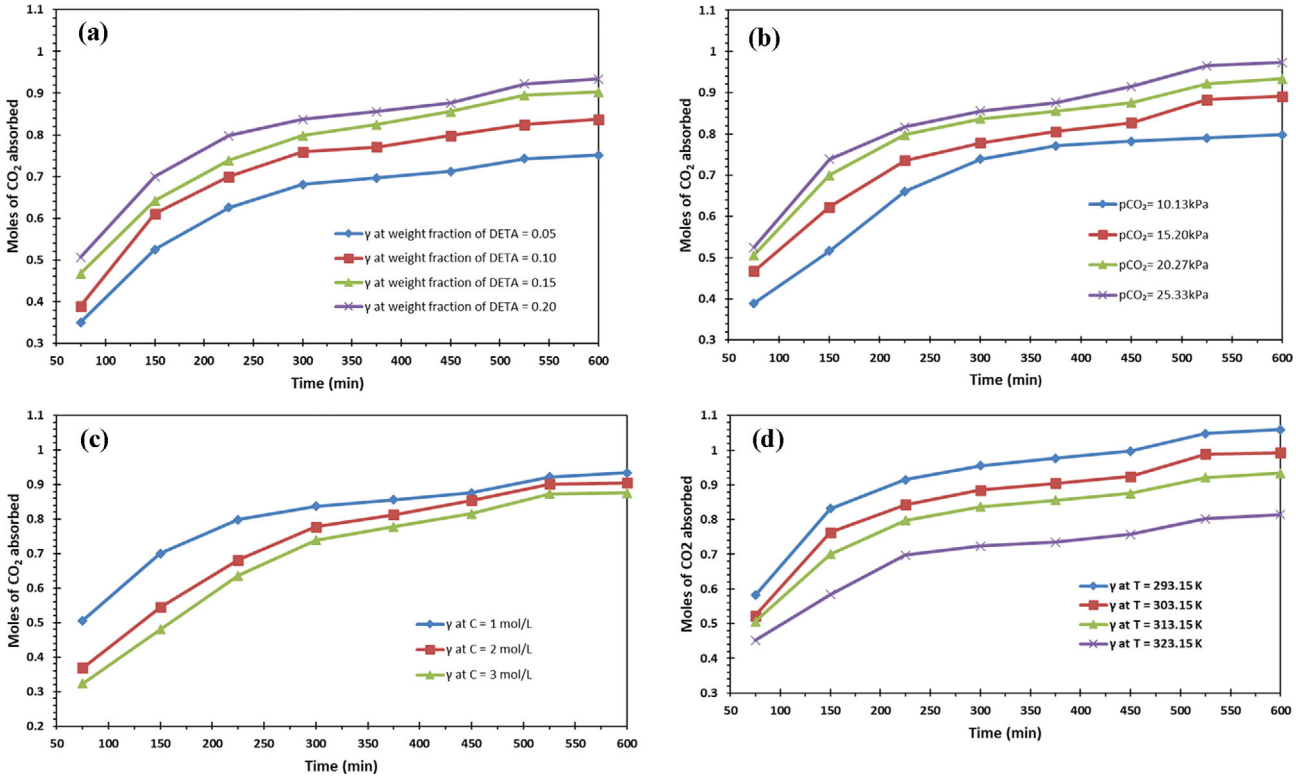

Fig. 4. CO_2 loading versus time with (a) different value of weight fraction of DETA (m_{DETA}) in total amine mixture at constant T 313.15 K, p_{CO_2} 20.27 kPa, and C 1 mol·L^{-1}, (b) distinct values of partial pressure of CO_2 (10.13-25.33 kPa) in the simuated gas stream at constant m_{DETA} 0.20, T 313.15 K, and C 1 mol·L^{-1}, (c) different values of total amine blend concentration (1, 2 and 3 mol·L^{-1}) at constant m_{DETA} 0.20, p_{CO_2} 20.27 kPa and T 313.15 K, (d) different values of temperature (293.15-323.15 K) at constant m_{DETA} 0.20, p_{CO_2} 20.27 kPa and C 1 mol·L^{-1}.

mol·L^{-1}) and keeping the other operating parameters constant, such as temperature at 313.15 K, partial pressure of CO_2 at 20.27 kPa and weight fraction of DETA in the absorbent blend at 0.20. This plot shows a decreasing pattern in CO_2 loading with increasing total amine blend concentration.

Fig. 4(d) shows the change in CO_2 loading with respect to absorption time at different values of temperature ranging from 293.15-323.15 K; in this regard, the other parameters were kept constant, such as total amine blend concentration of 1 mol·L^{-1}, partial pressure of CO_2 in the simulated gas stream at 20.27 kPa and weight fraction of DETA in the amine blend at 0.20. It can be concluded from the graph that as the temperature is enhanced, the CO_2 loading decreases. At the start of every experimental run, the dissolved gas increases for a while, and then it becomes constant as the aqueous amine mixture becomes saturated.

3. Development of an Empirical Model for Calculating Equilibrium CO_2 Loading in the Aqueous Amine Blend

To verify the experimental equilibrium CO_2 loading for the 3-DMA-1-P+DETA absorbent blend, an empirical model for calculating the equilibrium CO_2 loading in the amine solution was developed and is represented by Eq. (1). This equation consists of all the operating parameters which were used during the entire experiment. These factors include total amine blend concentration, CO_2 partial pressure in the simulated gas stream, activator DETA weight fraction, and temperature. All these parameters were used within a specified span, such as temperature in a span of 293.15-323.15 K, partial pressure of CO_2 in a span of 10.13-25.33 kPa, DETA weight fraction in a span of 0.05-0.20, and total concentration of amine blend in a span of 1-3 mol·L^{-1}.

$$\gamma_{cal}=A+Bm_{DETA}+Cm_{DETA}^2+Dp_{CO_2}+Ep_{CO_2}^2+FX+GX^2+HT+IT^2 \quad (1)$$

where γ is the equilibrium CO_2 loading in the aqueous 3-DMA-1-P+DETA solution (mol CO_2·mol amine^{-1}), p_{CO_2} is the partial pressure of CO_2 in the simulated gas stream (kPa), X is the total concentration of amine solution (mol·L^{-1}), T is the blend operating temperature (K), m_{DETA} is the DETA weight fraction in the amine blend of 3-DMA-1-P+DETA and A, B, C, D, E, F, G, H, I are the coefficients of the theoretical model. To find the equilibrium CO_2 loading by this model, coefficients were calculated with Excel Solver by using the experimental values under specified operating conditions. Calculated values of coefficients are listed in Table 4.

On using these coefficient values, along with other operating parameters, equilibrium CO_2 loading values were calculated, and final calculated values, along with the relative deviation between experimental and calculated values, are reported in Table 3. To calculate the percentage relative deviation (RD %) and percentage absolute average deviation (AAD %), the following formulas were used:

$$\%RD=\frac{|\gamma_{exp}-\gamma_{cal}|}{\gamma_{exp}}\times 100 \quad (2)$$

Table 4. Theoretical model coefficients and their corresponding values

Coefficient	Values	Coefficient	Values
A	−6.331733	F	−0.035059
B	2.444190	G	−0.003226
C	−5.210175	H	0.051914
D	0.015074	I	−0.000097
E	−0.000065		

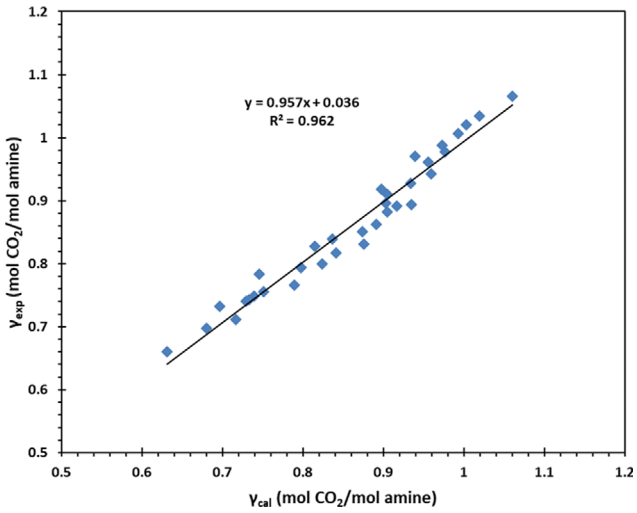

Fig. 5. Experimental CO_2 loading (γ_{exp}) versus calculated CO_2 loading (γ_{cal}) at equilibrium under specified operating condition.

$$\%AAD = \frac{1}{N} \times \Sigma_{i=1}^{N} \frac{|\gamma_{exp} - \gamma_{cal}|}{\gamma_{exp}} \times 100 \quad (3)$$

where, γ_{exp} represents the experimental equilibrium CO_2 loading, γ_{cal} is the equilibrium CO_2 loading calculated by the theoretical model and N is the number of experimental data points. To check the agreement of calculated values with experimental values, a plot for calculating the R^2 value was drawn between γ_{exp} and γ_{cal}. Fig. 5 depicts the R^2 value of 0.962, which shows that the developed model is reliable within identified operating conditions and is in agreement with the AAD of 2.10%, which is acceptable.

It is evident from Table 5 that equilibrium CO_2 loading in the amine blend of 3-DMA-1-P+DETA is higher in comparison with the other amine mixtures. So, it can be concluded that this amine blend gives promising results and can be used to capture CO_2 from coal-fired thermal power plants and other allied industries.

4. Calculation of Heat of Absorption for CO_2

Solvent selection for capturing CO_2 is mostly dependent upon the solvent regeneration cost, which is about 70-80% of the entire operating cost. Primary or secondary amines require a large amount of energy for the desorption step since it releases carbamate while reacting with CO_2, which takes high energy to break-down such species. Therefore, amine blends consisting of both types of amine solvents are in trend due to their fast kinetics, high CO_2 loading, low absorption capacity, low regeneration energy, and high thermal stability [6]. To reduce the overall operating cost, the solvent regeneration energy needs to be minimized, and it can be done by lowering the absorption heat of CO_2 because it is the main factor that impacts the solvent regeneration cost. Experimentally, the absorption heat of CO_2 can be estimated by using a calorimeter, and theoretically, it can be found by using the most popular Gibbs-Helmholtz equation, as shown below by Eq. (4):

$$\frac{d(\ln p_{CO_2})}{d\left(\frac{1}{T}\right)} = \frac{\Delta H_{abs}}{R} \quad (4)$$

where ΔH_{abs} is the heat of absorption of CO_2 or CO_2 absorption enthalpy in $kJ \cdot mol^{-1}$, p_{CO_2} is the partial pressure of CO_2 in the simulated gas stream in kPa, T is the system temperature in K, R is the universal gas constant ($R=8.314\ J \cdot mol^{-1}K^{-1}$). The above equation is in good agreement with the experimental results for absorption enthalpy and is shown by different researchers for different amine blends [55,60-62]. So it can be concluded from their work that the Gibbs-Helmholtz equation is quite good for calculating the heat of absorption of CO_2. To calculate the absorption enthalpy of CO_2 in the present amine blend of 3-DMA-1-P+DETA with the Gibbs-Helmholtz equation, a plot of $\ln(p_{CO_2})$ versus 1/T was drawn for constant values of CO_2 loading within the given conditions, as shown in Fig. 6. The value of the slope obtained from the graph was multiplied by the universal gas constant (R) to estimate the heat of absorption of CO_2.

Table 5. Comparison of loading values for different amine mixtures

Amine blend	C ($mol \cdot L^{-1}$)	T (K)	p_{CO_2} (kPa)	γ_{CO_2} (mol $CO_2 \cdot$mol amine^{-1})	Reference
3-DMA-1-P+DETA	1	313.15	20.27	0.934	Present work
3-DMA-1-P+DETA	2	303.15	20.27	0.956	Present work
3-DMA-1-P+DETA	3	313.15	20.27	0.876	Present work
3-DMA-1-P+DETA	1	313.15	15.20	0.891	Present work
MDEA+DEA	2	313	20	0.696	Kundu et al. [56]
DEEA+MEA	2.58	313	20	0.531	Luo et al. [58]
DEA+AEEA	2	303.15	20.27	0.740	Bajpai et al. [57]
MEA+3-DMA-1-P	1	313.15	15	0.547	Gao et al. [59]
MEA+MDEA	1	313.15	15	0.533	Gao et al. [59]
DEEA+AEEA	1	313.14	20.27	0.843	Shailesh et al. [25]

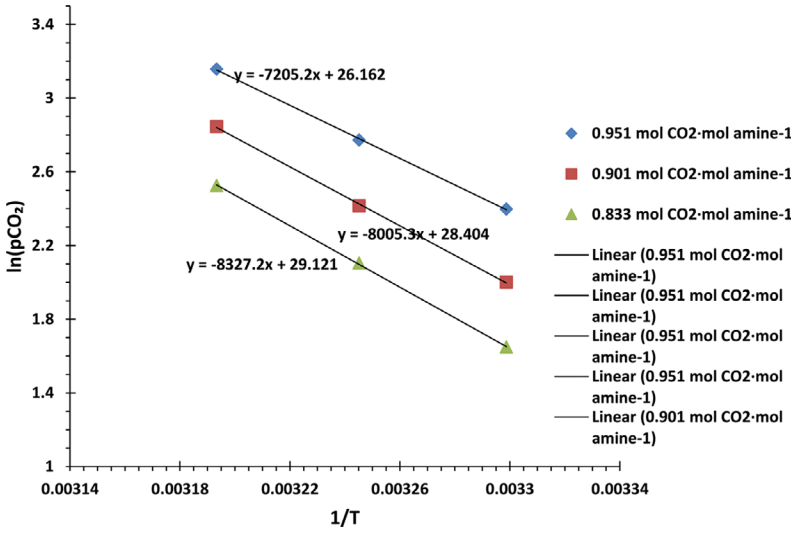

Fig. 6. Plot of $\ln(p_{CO_2})$ versus 1/T at different CO_2 loading values for calculating the heat of absorption of CO_2 at constant concentration of amine solution, C1 mol·L^{-1} and weight fraction of activator (m_{DETA}) 0.20.

The heat of absorption of CO_2 for different CO_2 loading values of 0.951 mol CO_2·mol $amine^{-1}$, 0.901 mol CO_2·mol $amine^{-1}$, and 0.833 mol CO_2·mol $amine^{-1}$ was −59.90 kJ·mol^{-1}, −66.55 kJ·mol^{-1}, and −69.23 kJ·mol^{-1}, respectively. It can be seen from the above plot that as CO_2 loading is increasing, the CO_2 absorption enthalpy value is slightly decreasing. The average value of heat of absorption of CO_2 is estimated to be −65.22 kJ·mol^{-1} for the present amine blend of 3-DMA-1-P+DETA, which is on the lower side as compared to the widely used benchmark amine MEA (−84.3 kJ·mol^{-1}) [75].

This absorption heat of CO_2 does not show the total heat cost, so to find the entire energy requirement for the present blend, the heat of vaporization and sensible heat need to be considered. The desorption step is opposite to that of the absorption process, so the value of heat of CO_2 desorption is the same as the heat of absorption of CO_2 with the opposite sign. So the value of heat of desorption for the present blend of 3-DMA-1-P+DETA is +65.22 kJ·mol^{-1}, which is lower than that of the conventional MEA (+84.3 kJ·mol^{-1}). For regeneration of the solvent, the heat duty for the desorption column (Q_{total}) depends on the desorption heat of CO_2 (ΔH_{des}), sensible heat (Q_{sens}), and heat of vaporization (Q_{vap}). This dependency is represented by the equation:

$$Q_{total}=\Delta H_{des}+Q_{vap}+Q_{sens} \quad (5)$$

Oyenekan et al. [63] concluded that Q_{sens} is small as compared to Q_{vap}, and Q_{vap} is mostly the same for all amine mixtures, so heat duty for desorption column depends on desorption heat of CO_2. So, a lower value of heat of absorption of CO_2 results in a lower value of heat duty. It means the energy required will be less because of the lower value of absorption heat of CO_2.

5. Response Surface Methodology (RSM) for Statistical Analysis–A Software-based Approach

RSM is a multivariable statistical approach for optimizing nearly all types of processes [41-43]. The goal of this method is to optimize the levels of the studied variables at the same time to achieve the best process performance [41]. It is widely used for modeling purposes and ultimately analyzes numerous problems [48].

In RSM, the objective function is dependent upon the regression model, and that function may be either first or second-order [40,45]. The regression model works as a tool for relating experimental work that establishes the relationship between two or more independent variables with the response as the dependent variable. In this present work, the objective function is the CO_2 loading that depends upon the four variables: temperature, the mole fraction of DETA, solution concentration, and partial pressure of CO_2. All these four variables are considered to be input variables, while the final response (CO_2 loading) is known as an output variable. It is crucial to select an experimental design that can be applied to the experimental set of data points before using RSM in operation [46].

The mathematical model used in RSM mostly relies on a quadratic type equation, in which the model selection, model equation, and their coefficient estimation are done by this mathematical tool. A quadratic model can be suggested as:

$$Y=\phi_0+\Sigma_{i=1}^{k}\varphi iXi+\Sigma_{i=1}^{k}\varphi iiXi^2+\Sigma\Sigma_{i<j}\varphi iiXiXj \quad (6)$$

where Y is the final response, φ_0 is the constant coefficient, φi is the linear constant coefficient, φii is the quadratic constant coefficient, and φij is the interaction coefficient. Furthermore, Xi and Xj are the independent encoded variables used during the entire experimental process. Eq. (6) predicts the behavior of the response in the experimental set of data points, which is described as a function of independent variables. All the results analysis of this model or model fitness is carried out by using analysis of variance (ANOVA) and lack-of-fit test [41].

5-1. Study of Equilibrium CO_2 Loading with Response Surface Methodology (RSM) and its Model Validation

Different experimental sets were created with RSM software of version Design Expert-8.0.7.1. In this software, quadratic mode and the central composite design type with 35 runs were under consideration. Table 6 indicates all four independent variables along

Table 6. Experimental independent variables and their coded levels used for central composite design

Independent variable	Symbol	Coded Levels				
		$-\alpha$	−1	0	+1	$+\alpha$
Temperature	A	278.15	293.15	308.15	323.15	338.15
Mole fraction of DETA	B	−0.025	0.05	0.13	0.20	0.275
Solution concentration	C	0	1.00	2	3.00	4
Partial pressure of CO_2	D	2.53	10.13	17.73	25.33	32.93

Table 7. Results of multiple regression analysis by ANOVA for the estimation of equilibrium CO_2 loading

Source	Sum of squares	df	Mean square	F value	p-Value Prob>F	
Model	0.39	12	0.033	85.94	<0.0001	Significant
A-Temperature	0.071	1	0.071	186.96	<0.0001	
B-Mole fraction of DETA	0.091	1	0.091	239.51	<0.0001	
C-Solution concentration	0.029	1	0.029	77.68	<0.0001	
D-Partial pressure of CO_2	0.070	1	0.070	184.41	<0.0001	
AB	1.023E-003	1	1.023E-003	2.70	0.1148	
AC	1.715E-005	1	1.715E-005	0.045	0.8336	
AD	0.000	0				
BC	7.602E-004	1	7.602E-004	2.00	0.1710	
BD	0.000	0				
CD	9.339E-004	1	9.339E-004	2.46	0.1310	
A^2	0.012	1	0.012	31.02	<0.0001	
B^2	3.470E-003	1	3.470E-003	9.14	0.0062	
C^2	2.836E-004	1	2.836E-004	0.75	0.3967	
D^2	8.256E-004	1	8.256E-004	2.18	0.1544	
Residual	8.349E-003	22	3.795E-004			
Cor total	0.40	34				
Lack of fit		22				
Pure error		0				

with their corresponding coded levels, as shown in the design summary.

The ANOVA indicates different factors like the degree of freedom (df) value, mean square value, F-value, P-value, etc. Model F-value, P-value, and values of A, B, C, D, A^2, and B^2 of the ANOVA suggest whether the chosen system model is significant or not. Table 7 indicates ANOVA analysis of equilibrium CO_2 loading as final response, and it also includes the results of fitting Eq. (6) with the experimental data. The model F-value from Table 7 was found to be 85.94, which implies that the model is significant. Similarly, values of Prob>F for all the independent variables should be less than 0.0500 for the model to be significant. If values are greater than 0.1000 in the case of A, B, C, D, A^2, and B^2 show the insignificance of the model, but in our case, all such values are less than 0.0001. Finally, from Eq. (6) on putting all the values of constants obtained from the ANOVA, then this final equation in terms of coded factors can be re-written as:

$$\text{Equilibrium } CO_2 \text{ loading} = 0.85 - 0.13A + 0.089B - 0.057C + 0.10D + 0.016AB + 1.813E\text{-}003AC + 8.802E\text{-}003BC + 0.014\,CD - 0.053A^2 - 0.029B^2 - 6.457E\text{-}003\,C^2 - 0.017\,D^2 \quad (7)$$

Table 8. Statistical parameters obtained from the analysis of variance (ANOVA) for the model of equilibrium CO_2 loading as a final response

Std. Dev.	0.019
Mean	0.86
C.V. %	2.27
PRESS	0.026
R-squared	0.9791
Adjusted R-squared	0.9677
Predicted R-square	0.9342
Adequate precision	33.476

The ANOVA analysis also provided statistical parameters like R-square value, adjusted R-square value, predicted R-square value, etc., and all are listed in Table 8. The R-square value is 0.9791, the adjusted R-square value is 0.9677, and the predicted R-square value is 0.9342. Adequate precision measures the signal-to-noise ratio, and if its ratio is greater than 4, then it is desirable, and in our case, it was found to be 33.476, which indicates an adequate signal, so the model can be used to navigate the design space. The model consists

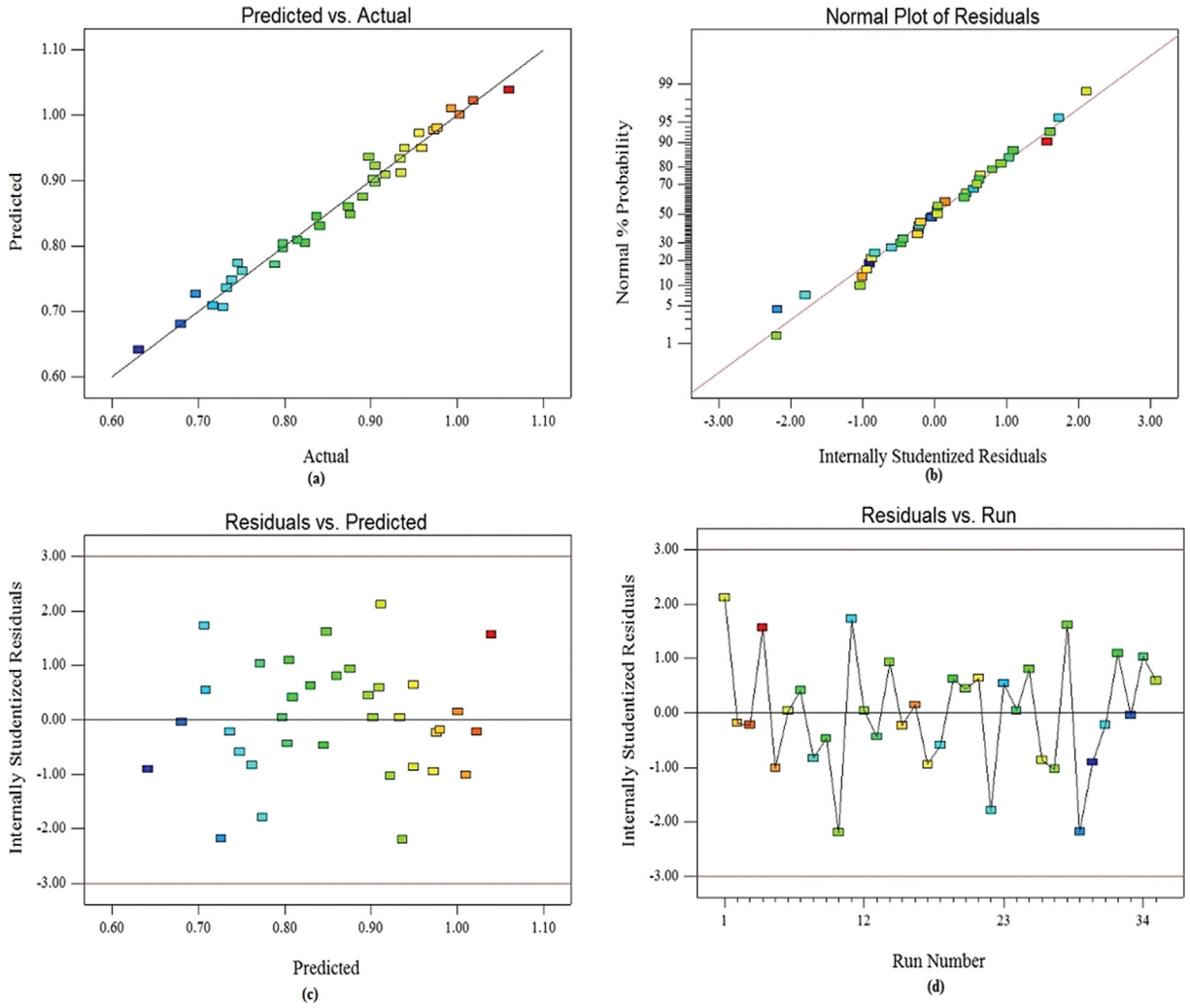

Fig. 7. (a) The actual versus predicted plot of equilibrium CO_2 loading, (b) The studentized residuals and normal percentage probability plot of equilibrium CO_2 loading, (c) The predicted equilibrium CO_2 loading and studentized residuals' plot, (d) Internally studentized residuals versus the run number for the equilibrium CO_2 loading.

of a coefficient of variation (CV %) of 2.27%, which simply means that there is a small standard deviation (SD) relative to the mean.

The predicted R-square value (0.9342) is in proper deal with the adjusted R-square value (0.9677), so these values validate the model. The actual calculated experimental data versus predicted data for the equilibrium CO_2 loading plot is shown in Fig. 7(a). The values obtained from the actual experiment were very much close to the predicted value, which is a clear indication that the developed model was successful in the calculation of equilibrium CO_2 loading. The normal % probability plot of residual is shown in Fig. 7(b). The residuals were generally distributed along a straight line, indicating a normal distribution of errors. The relationship between internally studentized residuals versus predicted equilibrium CO_2 loading is shown in Fig. 7(c). The randomly scattered plot indicates that the variance of original observations is constant for all the responses so obtained [48,51]. Fig. 7(d) indicates the internally studentized residuals versus the run number for the equilibrium CO_2 loading. This plot indicates that there was no proper relationship between the observed outputs and the order of the experimental set of data points. The plot of studentized residuals with temperature, mole fraction of DETA, solution concentration, and partial pressure of CO_2 is shown in Figs. 8(a), 8(b), 8(c), and 8(d), respectively. On analyzing all the various parameters, it is quite clear that CCD successfully passed all the statistical tests.

5-2. 3-D Surfaces and Contour Graphs Analysis

3-D surfaces and contour graphs are general representations of the chosen model for the study. It gives a clear idea of the effectiveness of independent variables and the final output response within the selected domain used for the entire analysis. Fig. 10(a) and (b) are the 3-D surface diagram and contour plot, respectively, that correlate the mole fraction of DETA (B), operating temperature (A), and final response (R1). It can be easily seen from the 3-D diagram that the response (R1-equilibrium CO_2 loading) increases with an increase in the mole fraction of DETA. Similarly, the response (R1) slightly increases with an increase in temperature, but after that it starts to decrease gradually by further increasing the temperature. Their reasons have also been discussed in the previous sections. Fig. 10(c) and (d) are the 3-D surface diagram and con-

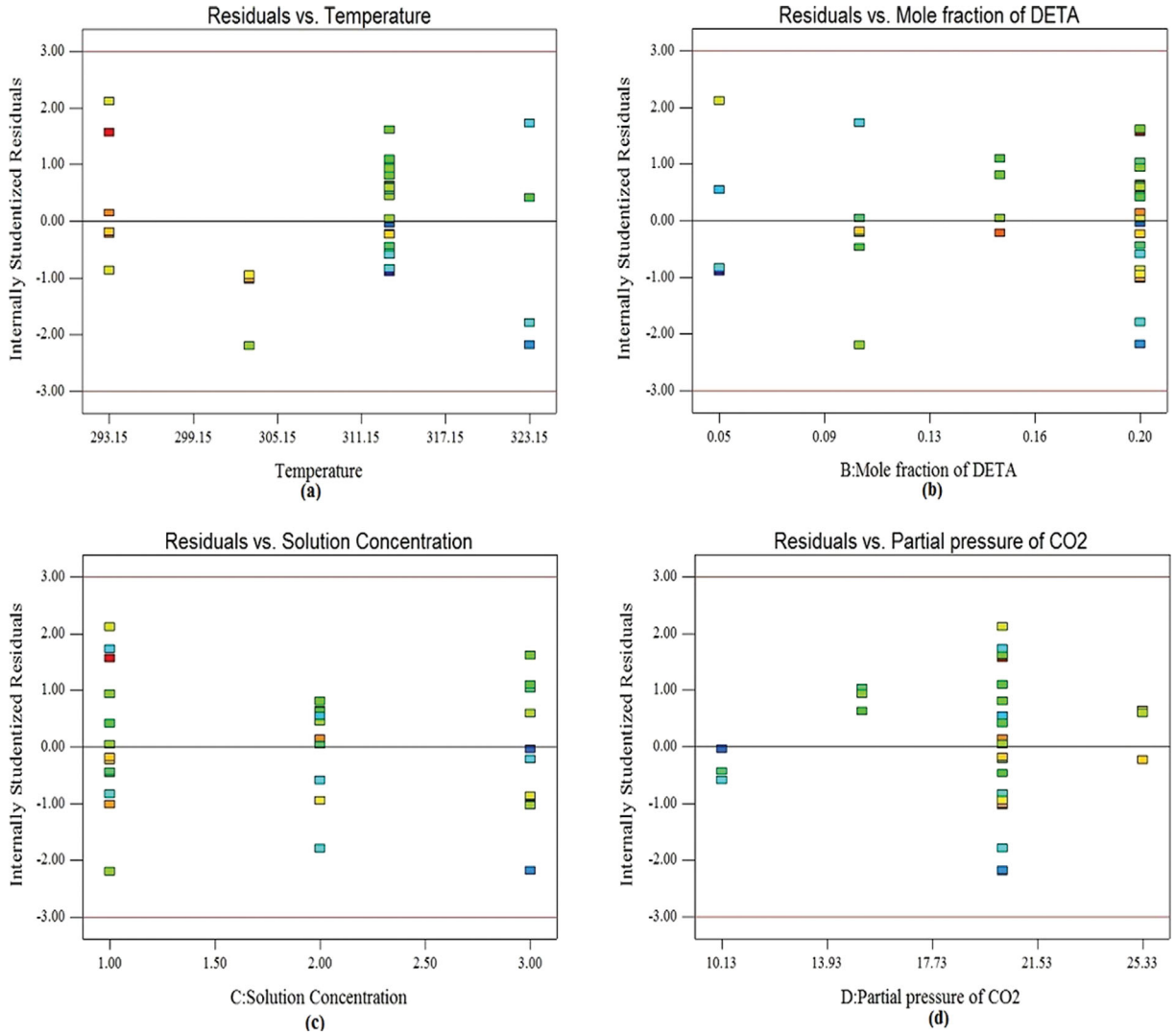

Fig. 8. (a) Plot of studentized residuals versus temperature for the ultimate response, (b) Plot of studentized residuals versus mole fraction of DETA for final response, (c) Plot of studentized residuals versus solution concentration for final response, (d) Plot of studentized residuals versus partial pressure of CO_2 for final response.

tour plot, respectively, that correlates solution concentration (C), temperature (A), and final response (R1). When the solution concentration is increased, the CO_2 loading as a final response increases to a certain limit, after which it begins to decrease. Likewise, the effect of temperature on the final response remains the same throughout the process that is discussed above. Fig. 11(a) and (b) are the 3-D surface diagram and contour plot, respectively, that show the relationship between partial pressure of CO_2 (D), temperature (A), and final response (R1). From the 3-D diagram and contour plot, it is evident that the response increases with an increase in partial pressure of CO_2 from the lower range to the higher range, and their reasons have been discussed in the previous sections. The effect of temperature remains constant throughout. Fig. 11(c) and (d) are the 3-D diagram and contour plot, respectively, that represent the correlations between mole fraction of DETA (B), solution concentration (C), and final response (R1). Similarly, Figs. 12 (a) and (b) show the 3-D surface and contour plot, respectively, and give the relationship between partial pressure of CO_2 (D), the mole fraction of DETA (B), and final response (R1). Finally, the 3-D surface and the contour plot of partial pressure of CO_2 (D), solution concentration (C), and final response (R1) are shown in Figs. 12(c) and (d), respectively. The reasons for the increase or decrease in values have also been discussed in the previous sections.

5-3. Prediction of the Optimum Value and its Verification by the RSM Software

The software-based approach is used to achieve the optimum values of different independent variables present in the entire experiment to maximize the equilibrium CO_2 loading. Table 9 shows the desired goal of all the input independent variables with respect to the final response (R1), and when all such variables and responses are combined, they create an overall desirability function that must be optimized. As shown in Fig. 9, the optimum condition at which the best equilibrium CO_2 loading was found to be at 294.15 K, the mole fraction of DETA (m_{DETA}) of 0.20, solution concentration (C) of 1.3, and partial pressure of CO_2 (p_{CO_2}) of 24.22 kPa. Under these

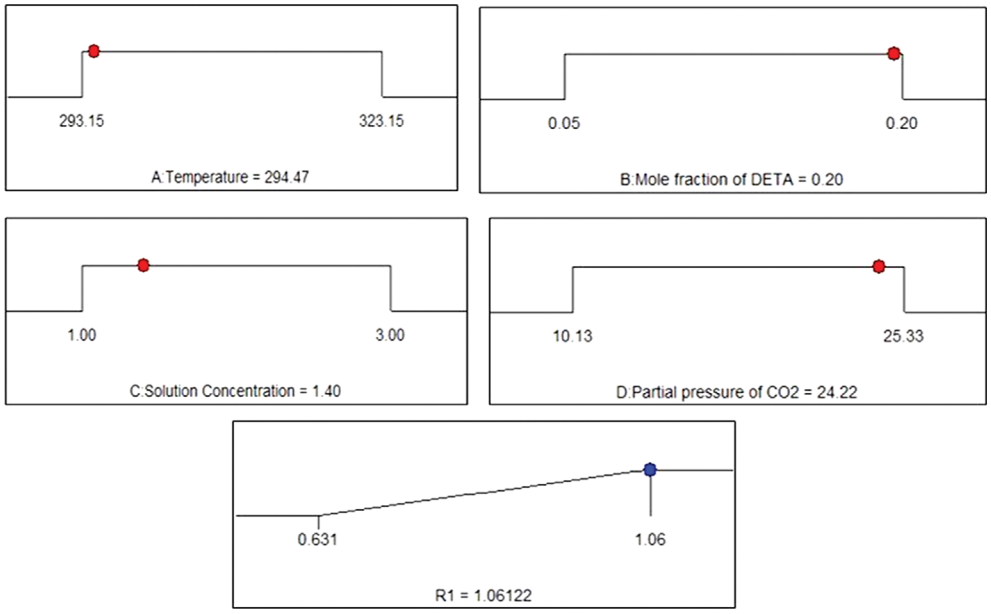

Fig. 9. Desirability ramp for the ultimate process response optimization.

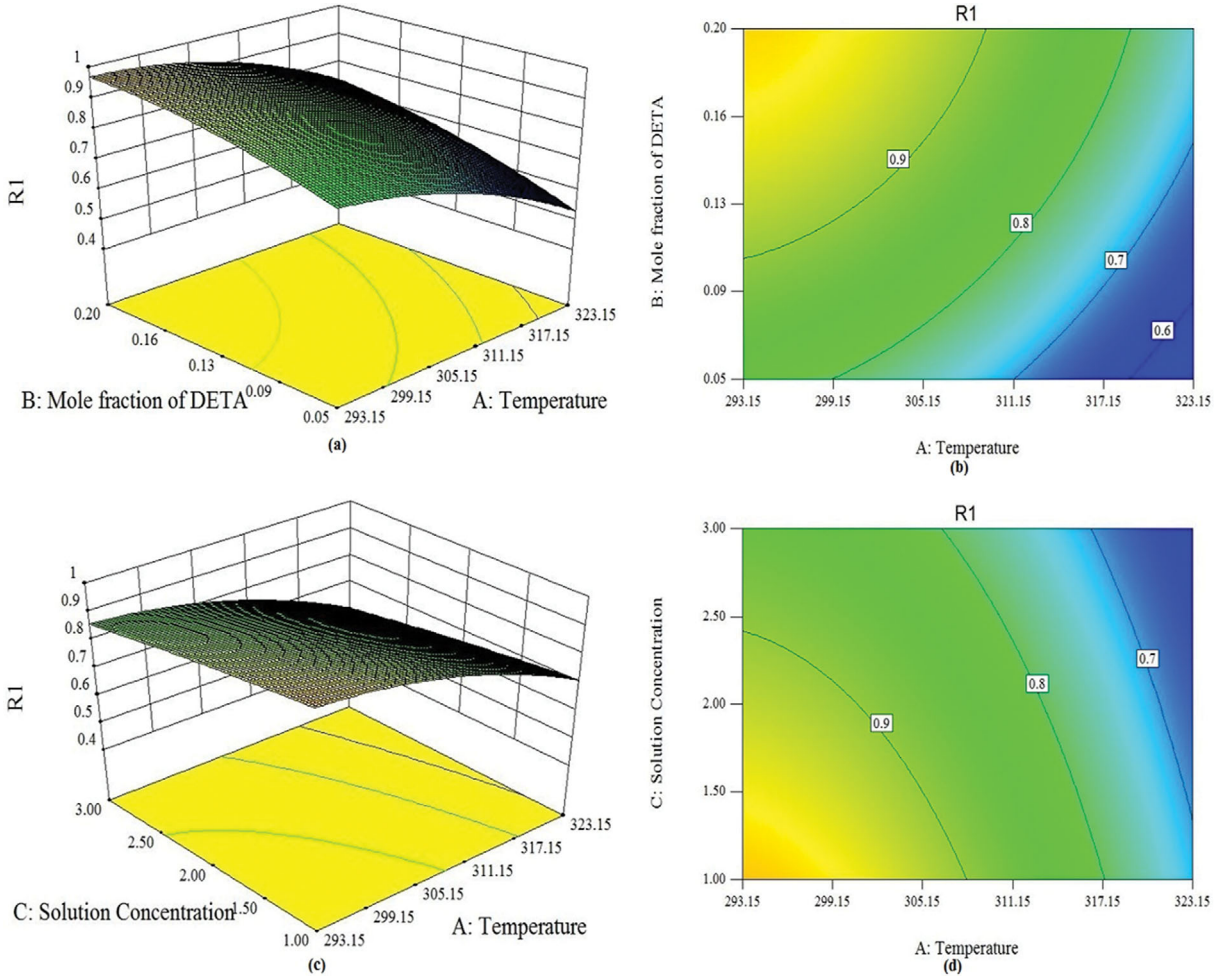

Fig. 10. (a) 3-D surface of mole fraction of DETA, temperature and final response, (b) Contour plots showing the effect of mole fraction of DETA, temperature and final response, (c) 3-D surfaces of solution concentration, temperature and final response, (d) Contour plots showing the effect of solution concentration, temperature and final response.

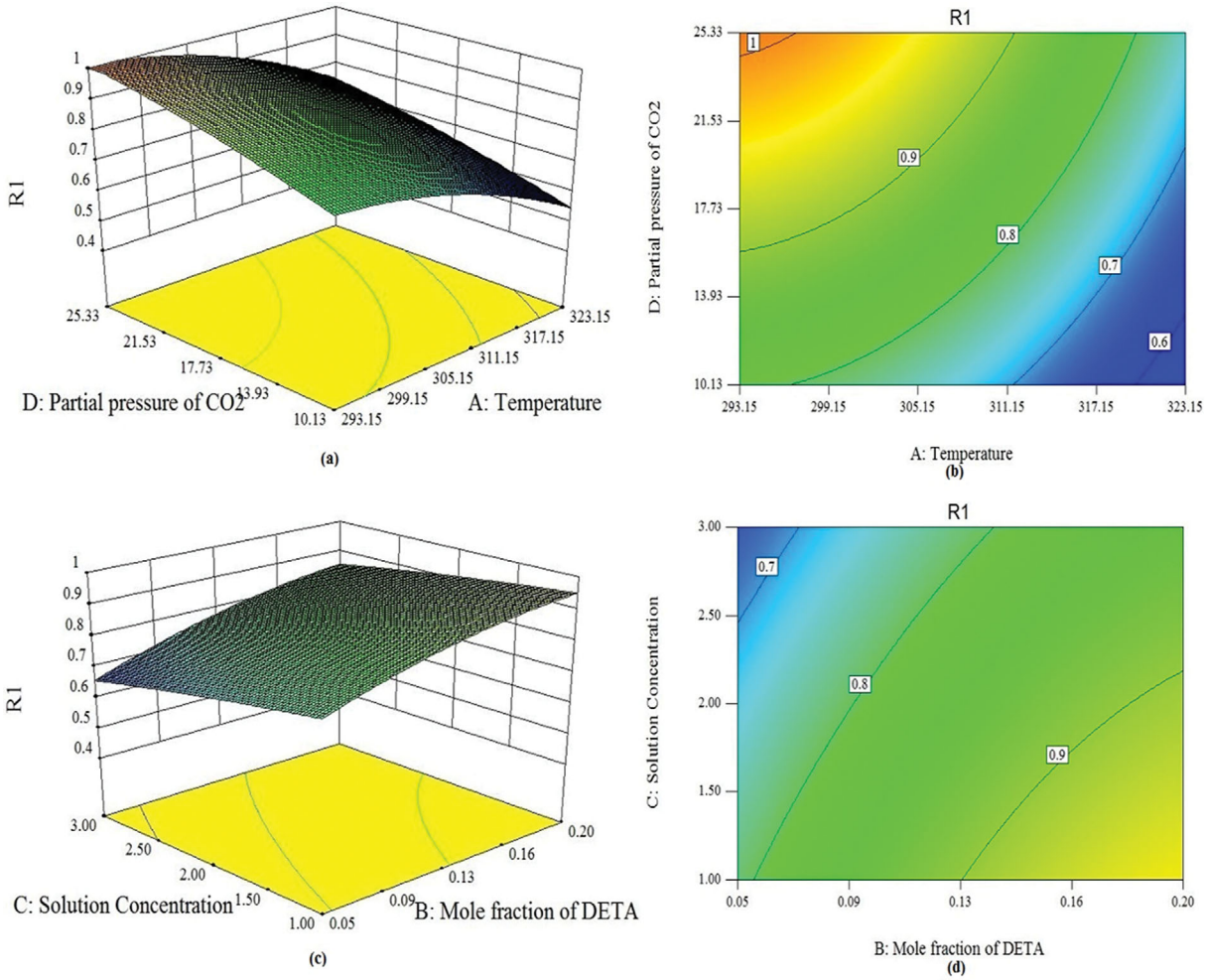

Fig. 11. (a) 3-D surface of partial pressure of CO_2, temperature and final response, (b) Contour plot showing the effect of partial pressure of CO_2, temperature and final response, (c) 3-D surface of mole fraction of DETA, solution concentration and final response, (d) Contour plot showing the effect of mole fraction of DETA, solution concentration and final response.

Table 9. Optimization of individual desirability responses in order to calculate the overall desirability response

Name	Goal	Lower limit	Upper limit	Lower weight	Upper weight	Importance
A: Temperature	Is in range	293.15	323.15	1	1	3
B: Mole fraction of DETA	Is in range	0.05	0.2	1	1	3
C: Solution concentration	Is in range	1	3	1	1	3
D: Partial pressure of CO_2	Is in range	10.13	25.33	1	1	3
R1	Maximize	0.631	1.06	1	1	3

optimum conditions, the final equilibrium CO_2 loading is predicted to be 1.068 as a final output. To verify the applicability of the selected model for the optimum equilibrium CO_2 loading, two solution concentrations close to the optimum value were examined. Two experiments were performed by changing solution concentration while keeping all other parameters to be constant. An average value of 1.0631 of equilibrium CO_2 loading was obtained, which is greater than 1% than that of the predicted value. This is a clear indication that our experiment performed satisfactorily with the predicted value by RSM software. Table 10 indicates the results of optimization of predicted values and actual values. Hence, it is a verification test to compare results between them.

CONCLUSION

The absorption performance of a novel aqueous amine blend of 3-DMA-1-P+DETA was studied to prove this as a potential solvent for CO_2 capture. The performance of this blend to capture CO_2 was checked experimentally in a bubble absorption column at various operating conditions. CO_2 loading with different concentra-

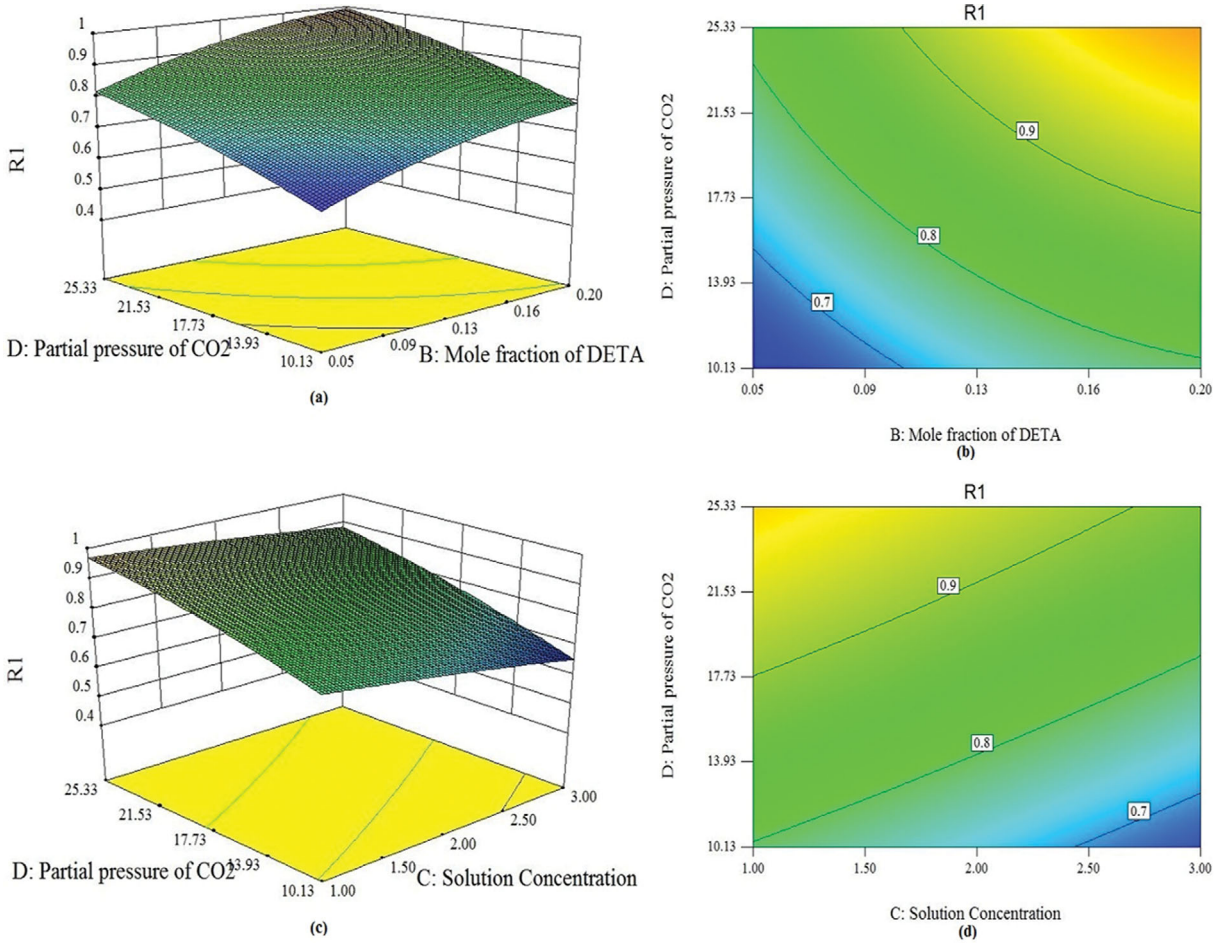

Fig. 12. (a) 3-D surface of partial pressure of CO_2, mole fraction of DETA and final response, (b) Contour plot showing the effect of partial pressure of CO_2, mole fraction of DETA and final response, (c) 3-D surface of partial pressure of CO_2, solution concentration and final response, (d) Contour plot showing the effect of partial pressure of CO_2, solution concentration and final response.

Table 10. Results of optimization based on the predicted value (RSM analysis) and actual value

	Temperature (K)	Mole fraction of DETA	Solution concentration ($mol \cdot L^{-1}$)	Partial pressure of CO_2 (kPa)	Equilibrium CO_2 loading (R1)
Predicted value	294.47	0.2	1.40	24.22	1.061
Actual value	294.15	0.2	1.50	24.22	1.059
Actual value	294.15	0.2	1.30	24.22	1.068

tions of amine mixture, partial pressure of CO_2, weight fraction of activator, and system temperature, was checked to obtain the optimum operating conditions. Also, the variation in CO_2 loading with absorption time was studied with the help of various plots.

As the weight fraction of DETA in the amine blend was increased from 0.05-0.20, there was an increase in the CO_2 loading. The change in the total concentration of the amine mixture from 1-3 $mol \cdot L^{-1}$ showed a sharp decrease in the value of equilibrium CO_2 loading. The equilibrium CO_2 loading started decreasing as the system temperature increased from 293.15-323.15 K. The increase in the partial pressure of CO_2 in the simulated gas mixture depicted a sharp rise in the value of CO_2 loading. At the best optimum operating condition of C=1 $mol \cdot L^{-1}$, m_{DETA}=0.20, T=313.15 K, p_{CO_2}=20.27 kPa, the value of CO_2 loading (γ_{exp}) was found to be 0.934 mol CO_2·mol $amine^{-1}$. A theoretical model to estimate CO_2 loading was developed to check the accuracy between the experimental and calculated values, and this model showed good agreement with the experimental data with a relative deviation of 2.10% (RD%), which is quite acceptable. The average value of heat of absorption of CO_2 was obtained to be -65.22 $kJ \cdot mol^{-1}$, which is lower in comparison to the standard MEA (−84.3 $kJ \cdot mol^{-1}$). To optimize the results, response surface methodology (RSM) was also used in the same ranges of parameters for temperature, mole fraction of DETA, partial pressure of CO_2, and solution concentration, as discussed above. Analysis of variance (ANOVA) was used to check the significance of the model chosen for the study. A second-order poly-

nomial model was used to obtain the optimized value of independent variables. Optimum equilibrium CO_2 loading was found to be 1.068 mol CO_2·mol amine^{-1} at T 294.15 K, m_{DETA} 0.20, C 1.3 mol/l, and p_{CO_2} 24.22 kPa. The comparison of equilibrium CO_2 loading values of this blend with other blends showed the ability of this blend to capture CO_2 through post-combustion technology.

ACKNOWLEDGEMENTS

The authors are very thankful for the encouragement given by the Indian Institute of Technology (Banaras Hindu University), Varanasi, and for the financial assistance furnished by the Ministry of Human Resource Development (MHRD), Government of India, for carrying out this present work.

NOMENCLATURE

AAD : absolute average deviation
ANOVA : analysis of variance
BBD : Box-Behnken design
C : amine blend concentration [mol/L]
CAS : chemical abstracts service
CCS : carbon capture & storage
CCD : central composite design
CO_2 : carbon dioxide
CH_4 : methane
DETA : diethylenetriamine
DMAP : 3-dimethylamino-1-propanol
HCL : hydrochloric acid
HTU : height of transfer unit
HFCs : hydro fluorocarbons
MDEA : methyldiethanolamine
MEA : monoethanolamine
N : No. of data points
N_2 : nitrogen
N_2O : nitrous oxide
NO_X : nitrogen oxide
PZ : piperazine
R : universal gas constant [J/mol·K]
RD : relative deviation
RSM : response surface methodology
SO_X : sulphur oxide
TEA : Triethanolamine
VLE : vapor-liquid equilibrium
p_{CO_2} : partial pressure of CO_2 [kPa]
m_{DETA} : weight fraction of DETA
γ_{exp} : experimental equilibrium CO_2 loading [molCO_2/molamine]
γ_{cal} : theoretical equilibrium CO_2 loading [molCO_2/molamine]
G^E : excess Gibbs energy
ΔH_{rxn} : heat of reaction [kJ/mol]
T : temperature [K]

REFERENCES

1. C. H. Yu, H. H. Cheng and C. S. Tan, *Int. J. Greenh. Gas Control*, **9**, 136 (2012).
2. M. Zaman and J. H. Lee, *Korean J. Chem. Eng.*, **30**, 1497 (2013).
3. A. A. Olajire, *Energy*, **35**, 2610 (2010).
4. J. Zhang, O. Nwani, Y. Tan and D. W. Agar, *Chem. Eng. Res. Des.*, **89**, 1190 (2011).
5. A. Gautam and M. K. Mondal, *Fuel*, **331**, 125864 (2023).
6. J. Zhang, Y. Qiao, W. Wang, R. Misch, K. Hussain and D. W. Agar, *Energy Procedia*, **37**, 1254 (2013).
7. A. Mukhtar, S. Saqib, N. B. Mellon, M. Babar, S. Rafiq, S. Ullah, M. A. Bustam, A. G. Al-Sehemi, N. Muhammad and M. Chawla, *J. Nat. Gas Sci. Eng.*, **77**, 103203 (2020).
8. M. H. Youn, K. T. Park, Y. H. Lee, S. P. Kang, S. M. Lee, S. S. Kim, Y. E. Kim, Y. N. Ko, S. K. Jeong and W. Lee, *J. CO2 Util.*, **34**, 325 (2019).
9. I. Ghiat, F. Mahmood, R. Govindan and T. Al-Ansari, *Energy Convers.Manag.*, **228**, 113668 (2021).
10. M. Bailera, P. Lisbona, B. Peña and L. M. Romeo, *J. CO2 Util.*, **46**, 101456 (2021).
11. P. Bains, P. Psarras and J. Wilcox, *Prog. Energ. Combust.*, **63**, 146 (2017).
12. M. C. Romano, R. Anantharaman, A. Arasto, D. C. Ozcan, H. Ahn, J. W. Dijkstra, M. Carbo and D. Boavida, *Energy Procedia*, **37**, 7176 (2013).
13. M. Kanniche, R. Gros-Bonnivard, P. Jaud, J. Valle-Marcos, J. M. Amann and C. Bouallou, *Appl. Therm. Eng.*, **30**, 53 (2010).
14. N. Zhong, H. Liu, X. Luo, M. J. AL-Marri, A. Benamor, R. Idem, P. Tontiwachwuthikul and Z. Liang, *Ind. Eng. Chem. Res.*, **55**, 7307 (2016).
15. C. Li, H. Liu, M. Xiao, X. Luo, H. Gao and Z. Liang, *Int. J. Greenh. Gas Control*, **63**, 77 (2017).
16. O. D. Araújo and J. L. de Medeiros, *Curr. Opin.Chem. Eng.*, **17**, 22 (2017).
17. M. Afkhamipour, M. Mofarahi and C. H. Lee, *Fluid Phase Equilib.*, **473**, 50 (2018).
18. B. Liu, M. Zhang, X. Yang and T. Wang, *J. Taiwan Inst. Chem. Eng.*, **103**, 67 (2019).
19. L. H. Lee, K. Im, S. Han, S. J. Yoo, J. Kim and J. H. Kim, *Sep. Purif. Technol.*, **250**, 117065 (2020).
20. K. Fu, G. Chen, T. Sema, X. Zhang, Z. Liang, R. Idem and P. Tontiwachwuthikul, *Chem. Eng. Sci.*, **100**, 195 (2013).
21. W. L. Theo, J. S. Lim, H. Hashim, A. A. Mustaffa and W. S. Ho, *Appl. Energy*, **183**, 1633 (2016).
22. S. K. Wai, C. Nwaoha, C. Saiwan, R. Idem and T. Supap, *Sep. Purif. Technol.*, **194**, 89 (2018).
23. X. Zhang, K. Fu, Z. Liang, W. Rongwong, Z. Yang, R. Idem and P. Tontiwachwuthikul, *Fuel*, **136**, 261 (2014).
24. C. Nwaoha, C. Saiwan, T. Supap, R. Idem, P. Tontiwachwuthikul, W. Rongwong, M. J. Al-Marri and A. Benamor, *Int. J. Greenh. Gas Control*, **53**, 292 (2016).
25. S. Kumar, R. Padhan and M. K. Mondal, *J. Chem. Eng. Data*, **65**, 523 (2020).
26. A. Wilk, L. Wieclaw-solny, A. Tatarczuk, A. Krotki, T. Spietz and T. Chwola, *Korean J. Chem. Eng.*, **34**, 2275 (2017).
27. A. Hartono, E. F. da Silva and H. F. Svendsen, *Chem. Eng. Sci.*, **64**, 3205 (2009).
28. A. Hartono, K. A. Hoff, T. Mejdell and H. F. Svendsen, *Energy Pro-*

cedia, **4**, 179 (2011).
29. K. A. Doyle, L. J. Murphy, Z. A. Paula, M. A. Land, K. N. Robertson and J. A. C. Clyburne, *Ind. Eng. Chem. Res.*, **54**, 8829 (2015).
30. M. Sheng, C. Xie, X. Zeng, B. Sun, L. Zhang, G. Chu, Y. Luo, J. F. Chen and H. Zou, *Fuel*, **234**, 1518 (2018).
31. L. Liu, X. Li, Z. Zhang, L. Li, Y. Bi and L. Zhang, *Greenh. Gases: Sci. Technol.*, **9**, 349 (2019).
32. A. V. Rayer and A. Henni, *Ind. Eng. Chem. Res.*, **53**, 4953 (2014).
33. Z. Idris, J. Chen and D. A. Eimer, *J. Chem. Thermodyn.*, **97**, 282 (2016).
34. T. W. Wu, Y. T. Hung, M. T. Chen and C. S. Tan, *Sep. Purif. Technol.*, **186**, 309 (2017).
35. S. Kadiwala, A. V. Rayer and A. Henni, *Chem. Eng. J.*, **179**, 262 (2012).
36. I. M. Bernhardsen and H. K. Knuutila, *Chem. Eng. Sci.* X, **3**, 100032 (2019).
37. D. Nath and A. Henni, *Ind. Eng. Chem. Res.*, **59**, 14625 (2020).
38. S. Singh, D. Pandey and M. K. Mondal, *J. Chem. Eng. Data*, **66**, 740 (2021).
39. A. Belabbaci, N. C. B. Ahmed, I. Mokbel and L. Negadi, *J. Chem. Thermodyn.*, **42**, 1158 (2010).
40. A. Nuchitprasittichai and S. Cremaschi, *Ind. Eng. Chem. Res.*, **52**, 10236 (2013).
41. S. Garcia, M. V. Gil, C. F. Martín, J. J. Pis, F. Rubiera and C. Pevida, *Chem. Eng. J.*, **171**, 549 (2011).
42. Q. Tang, Y. B. Lau, S. Hu, W. Yan, Y. Yang and T. Chen, *Chem. Eng. J.*, **156**, 423 (2010).
43. S. Sahraie, H. Rashidi and P. Valeh-e-Sheyda, *Process Saf. Environ.*, **122**, 161 (2019).
44. A. Hemmati and H. Rashidi, *Process Saf. Environ.*, **121**, 77 (2019).
45. A. Nuchitprasittichai and S. Cremaschi, *Comput. Chem. Eng.*, **35**, 1521 (2011).
46. M. V. Gil, M. Martínez, S. Garcia, F. Rubiera, J. J. Pis and C. Pevida, *Fuel Process Technol.*, **106**, 55 (2013).
47. C. Song, Y. Kitamura and S. Li, *J. Taiwan Inst. Chem. Eng.*, **45**, 1666 (2014).
48. D. Das and B. C. Meikap, *J. Environ. Sci. Health A*, **52**, 1164 (2017).
49. M. Saeidi, A. Ghaemi, K. Tahvildari and P. Derakhshi, *J. Chin. Chem. Soc.*, **65**, 1465 (2018).
50. A. Hemmati, H. Rashidi, A. Hemmati and A. Kazemi, *J. Nat. Gas Sci. Eng.*, **62**, 101 (2019).
51. P. Asgarifard, M. Rahimi and N. Tafreshi, *J. Chem. Eng.*, **99**, 601 (2021).
52. F. Y. Jou, F. D. Otto and A. E. Mather, *Ind. Eng. Chem. Res.*, **33**, 2002 (1994).
53. J. H. Choi, Y. E. Kim, S. C. Nam, S. H. Yun, Y. I. Yoon and J. H. Lee, *Korean J. Chem. Eng.*, **33**, 3222 (2016).
54. K. P. Shen and M. H. Li, *J. Chem. Eng. Data*, **37**, 96 (1992).
55. J. Lee, Y. K. Hong and J. K. You, *Korean J. Chem. Eng.*, **34**, 1840 (2017).
56. M. Kundu and S. S. Bandyopadhyay, *Fluid Phase Equilib.*, **248**, 158 (2006).
57. A. Bajpai and M. K. Mondal, *J. Chem. Eng. Data*, **58**, 1490 (2013).
58. S. Kumar and M. K. Mondal, *Korean J. Chem. Eng.*, **35**(6), 1335 (2018).
59. H. Gao, Z. Wu, H. Liu, X. Luo and Z. Liang, *Energ. Fuel*, **31**, 13883 (2017).
60. J. I. Lee, F. D. Otto and A. E. Mather, *J. Chem. Eng. Data*, **17**, 465 (1972).
61. S. W. Rho, K. P. Yoo, L. S. Lee, S. C. Nam, J. E. Son and B. M. Min, *J. Chem. Eng. Data*, **42**, 1161 (1997).